Jurnal Teknologi Reaktor Nuklir

Tri Dasa Mega

Journal homepage: jurnal.batan.go.id/index.php/tridam

Computational Fluid Dynamics Simulation of Temperature Distribution and Flow Characterization in a New Loop Heat Pipe Model

Muhammad Mika Ramadhani Restiawan[1], Mukhsinun Hadi Kusuma[2*], Khoiri Rozi[1], Berkah Fajar Tamtomo Kiono[1], Muhammad Yunus[2], Alif Rahman Wirza[1], Yoyok Dwi Setyo Pambudi[2], Sofia Loren ButarButar[2], Giarno[2], Sumantri Hatmoko[2]

[1]Department of Mechanical Engineering, Diponegoro University, Jl. Prof. Sudharto, S.H., Tembalang-Semarang 50275, Indonesia
[2]Research Center for Nuclear Reactor Technology, National Research and Innovation Agency, Kawasan Sains Terpadu B.J. Habibie, Serpong, Tangerang Selatan 15314, Indonesia

ARTICLE INFO

Article history:

Received: April 25th, 2024
Received in revised form: May 16th, 2024
Accepted: May 20th, 2024

Keywords:

Temperature distribution
Flow characterization
Computational fluid dynamic
Loop heat pipe
Passive cooling system

A B S T R A C T

The loop heat pipe (LHP) is being considered for passive cooling systems in nuclear installations. A combined approach of simulation and experimentation is essential for achieving comprehensive knowledge of the LHP. Research on the LHP using Computational Fluid Dynamics (CFD) is necessary to understand phenomena that are challenging to ascertain experimentally. This study examines the temperature distribution and flow characteristics in a new LHP model. The method used in this research is simulation using CFD Ansys FLUENT software. In the simulation, the LHP has an inner diameter of 0.1016 m. This LHP features a wick made from a collection of capillary pipes without a compensation chamber. Demineralized water is used as the working fluid with a filling ratio of 100% of evaporator volume. The hot water temperature in the evaporator section is set at 70 °C, 80 °C, and 90 °C. The temperature on the outer surface of the condenser pipe is determined using experimental temperature inputs. An inclination angle of 5° and an initial pressure of 12,100 Pa are applied to LHP. The CFD simulation results show that the temperature distribution profile under steady-state conditions in the loop heat pipe appears almost uniform. The temperature difference between the evaporator and condenser remains consistent. The flow of working fluid in the LHP is driven by buoyancy forces and fluid flow, allowing the working fluid in the LHP to flow in two phases from the evaporator to the condenser and then condensate from the condenser back to the evaporator. In conclusion, the temperature distribution and flow patterns in the LHP are consistent with common phenomena observed in heat pipes. This modeling can be used to determine the profiles of temperature distribution and flow in LHP of the same dimensions under various thermal conditions.

1. INTRODUCTION

As human life evolves in tandem with modernity, the necessity for energy becomes crucial to support various activities. The availability of energy significantly enhances progress across multiple domains, including industry, education,

*Corresponding author
E-mail: mhad001@brin.go.id
DOI: 10.55981/tdm.2024.7054

transportation, and technology [1]. The availability of energy plays a crucial role in improving societal welfare. The increasing energy demands of communities coincide with the depletion of non-renewable energy sources, such as coal, natural gas, and petroleum. As reserves of non-renewable energy diminish and environmental concerns associated with their extraction escalate, there is a heightened urgency to transition towards renewable energy sources [2].

Nuclear energy is considered a renewable energy source with the potential to replace the use of fossil fuels [3]. It is a promising alternative electricity generation system with significant potential [4]. Nuclear Power Plants can consistently provide electricity generation without emitting carbon gases [5]. Nuclear energy offers the advantage of generating large-scale, cost-effective, and stable electrical capacity [6]. However, the use of nuclear energy also comes with significant potential risks.

There are various drawbacks associated with the utilization of nuclear energy. Following energy generation, nuclear power results in radioactive waste that requires careful management [7]. Moreover, the risk of explosions at nuclear power plant is recognized as one of the most significant disadvantages of nuclear energy utilization. The Fukushima Dai-ichi Nuclear Power Plant accident on March 11, 2011, exemplifies the hazard associated with nuclear industrial incidents. In this event, an earthquake followed by a tsunami disabled the generator that powered the equipment needed to cool the reactor. This led to heat accumulation and ultimately a reactor explosion. After this disaster, researchers began to focus on preventing similar incidents, which spurred advancements in nuclear technology, including the development of passive cooling systems in reactors. These systems are designed to function without external energy sources in case of active safety system failures [8].

Studies initiated after the incident underscore the importance of passive cooling in nuclear power plants to prevent future disasters. One approach involves the use of Loop Heat Pipe (LHP) [9]. The implementation of LHP is expected to passively transfer heat when electrical power in nuclear power plants fails, thereby minimizing the risk of explosion. The development of LHP technology is widely utilized in the fields of aeronautics and electronics as a media for passive cooling [10]. The primary advantage of LHP lies in its ability to transport heat efficiently over long distances through phase change of the working fluid [11]. A literature review indicates that LHPs have the potential for application in passive cooling systems within nuclear installations [12].

However, an obstacle encountered in experimental studies of LHP is understanding the thermo-hydraulic mechanisms involved. These mechanisms are challenging to predict because heat and mass transfer processes occur in two phases during the operation of the heat pipe [13]. The computational fluid dynamics (CFD) method is used to determine the two-phase flow characteristics and heat transfer processes within a heat pipe [14]. Through CFD simulations, heat transfer phenomena can be captured more clearly and the results obtained from CFD calculations can be validated using experimental data.

In relation to the research on LHP that have the potential to be used as passive cooling systems in nuclear installations, the Research Organization for Nuclear Energy, National Research and Innovation Agency of Indonesia, is currently conducting research on experimental models of LHP. These models use a set of capillary pipes with a wick but without a compensation chamber. The experiments being conducted require support from CFD. The results obtained from CFD will be utilized to understand phenomena that are difficult to obtain experimentally.

The approach employed in this study involves conducting simulations using CFD Ansys FLUENT software. During the simulation process, the LHP is defined with an inner diameter of 0.1016 m. The wick of this LHP consists of capillary pipes without a compensation chamber. Demineralized water serves as the working fluid, completely filling the evaporator volume. Hot water temperatures of 70 °C, 80 °C, and 90 °C are applied as temperature sources in the evaporator section. Experimental temperature inputs are used to determine the temperature on the outer surface of the condenser section. An inclination angle of 5° and an initial pressure of 12,100 Pa are applied to the LHP.

2. METHODOLOGY

In general, CFD simulation procedure consists of three main stages: Pre-Processing, Processing, and Post-Processing. Pre-Processing is the initial phase of CFD simulation, involving tasks such as geometry creation, mesh generation, boundary plane definition on the geometry, and mesh verification. Processing encompasses activities related to boundary condition determination, performing numerical calculations, and executing iterative procedures. Post-Processing includes the generation of temperature distribution plots and volume fraction visualization [15].

2.1 Governing Equation of CFD

The Volume of Fluid (VOF) technique is designed for scenarios involving two or more non-mixable working fluids. It aims to precisely determine the interface position between these fluids or phases, with particular emphasis on both transient and steady-state gas/liquid interfaces [16]. The governing equations the VOF model are as follows.

A. Continuity Equation

The continuity equation for the vapor phase is defined as follows [16].

$$\frac{\partial \rho}{\partial t} + \nabla \cdot (\rho \vec{v}) = S_m \tag{2.1}$$

B. Momentum Equation

The momentum equation is defined as follows [16].

$$\frac{\partial}{\partial t}(\rho \vec{v}) + \nabla \cdot (\rho \vec{v} \vec{v}) = -\nabla p + \nabla \cdot [\mu(\nabla \vec{v} + \nabla \vec{v}^T)] + \rho \vec{g} + \boldsymbol{S}_{\mathrm{CSF}} \tag{2.2}$$

C. Energy Equation

Energy equation in the volume of fluid (VOF) form is presented as the following [16].

$$\frac{\partial}{\partial t}(\rho \boldsymbol{C_p T}) + \nabla \cdot [(\rho \boldsymbol{C_p T} + \boldsymbol{p})\vec{v}] = \nabla(\boldsymbol{k} \nabla \boldsymbol{T}) + \boldsymbol{S_E} \tag{2.3}$$

2.2 The LHP Geometry and Mesh

A full scale 2D geometry of the LHP was built in Ansys DesignModeler software. The LHP has a height of 1.1521 m and a width of 0.801 m, with four elbows each having a radius of 0.1524 m. The heat pipe comprises three sections, namely the evaporator, adiabatic, and condenser.

The evaporator section has a length of 1.850 mm, with a horizontal length of 0.75 m and a vertical length of 0.3 m. This section is submerged in a tank containing hot water during the experiment, where heat from the water is absorbed by the evaporator section.

The adiabatic section consists of two distinct parts and is installed vertically. The right adiabatic section has a length of 0.7 m. It does not contain a wick and allows the vapor path to rise to the condenser section. The left adiabatic section includes a capillary pipe as a wick, which functions to restrain the upward movement of vapor and facilitates the return path of condensate to the evaporator section. Additionally, the placement of the wick also serves to maintain the LHP's natural cycling.

The condenser section has a length of 1.27 m, with a horizontal height of 0.75 m and a vertical height of 0.2 m. The condenser is responsible for heat absorption, where in the experiment, the heat transfer process occurs through forced convection from the airflow generated by a fan. The geometry of the LHP used in this simulation can be seen in Fig. 1.

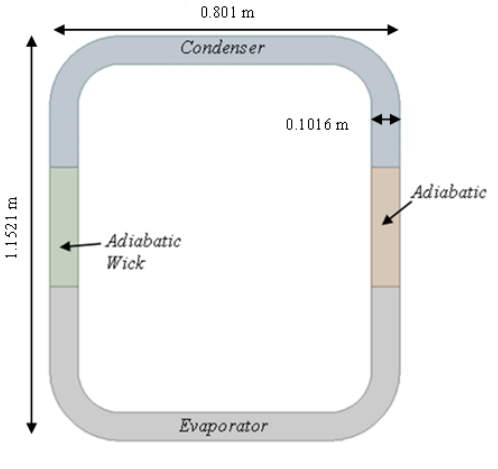

Fig. 1. Geometry model of new LHP.

In this simulation, the automatic method for mesh shape is selected with inflations; however, the sizing for the mesh is done manually. The minimum and mesh sizes are chosen to be 0.002 m as shown in Fig. 2. Various mesh sizes were tested to achieve mesh independence, as shown in Table 1. The final grid number of the fluid domain was 119,512. The results of grid independence test can be seen in Fig. 3 and 4.

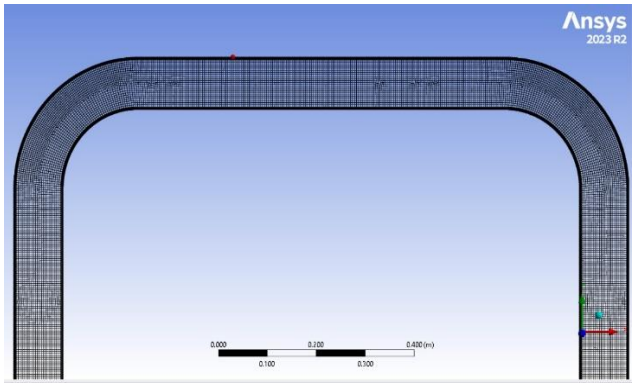

Fig. 2. Mesh model of LHP system

Table 1. Grid Independence Result

Mesh	Grid 1	Grid 2	Grid 3
	119512	53069	29577
T_{Evap} AVG (℃)	78.13	78.15	78.08
T_{Cond} AVG (℃)	66.36	66.34	66.23

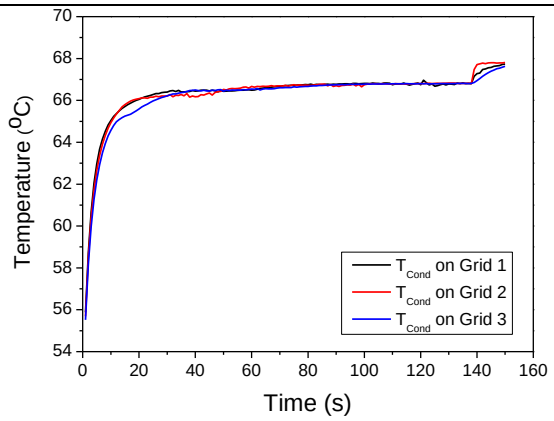

Fig. 3. Grid independence test in condenser

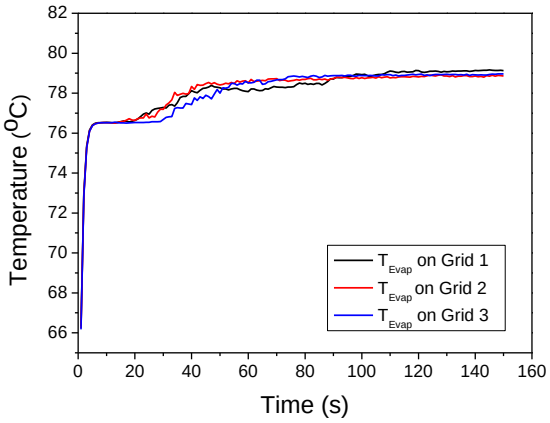

Fig. 4. Grid independence test in evaporator

2.4 CFD Setup

In this simulation, a Pressure-based solver was used. Gravity was activated with values of -9.77 m^2/s at the Y-axis and -0.84 m^2/s at the X-axis to simulate a 5° inclination [17]. The energy model was activated to include thermal effects in the simulation. The multiphase model used the Volume of Fluid (VoF) approach and activated implicit body force [18]. The viscous model employed the k-epsilon model, which was used to simulate natural circulation for loop geometry [19]. Water in liquid and vapor forms was selected from the FLUENT database for the liquid phase and copper for the solid material. Liquid water is the primary phase, while water vapor is the secondary phase. The inter-phase surface tension was set as a constant value of 0.072 N/m. Temperature variations on the outer wall of the evaporator were set at 70 °C, 80 °C, and 90 °C to simulate the heat from the pool. The temperature on the outer wall of the condenser used a user-defined profile obtained from the experiment, while the adiabatic section was set to zero flux, assuming that this section is isolated. The filling ratio in this simulation was 100% of the evaporator volume, with the initial operating pressure set at 12,100 Pa to achieve a saturation temperature of 47 °C. Porous media, an input parameter in Ansys FLUENT, can be utilized in both single-phase and double-phase applications. This modeling approach is employed for applications such as modeling filter papers, perforated plates, and arrays of small tubes. In this simulation, porous media was used to simulate a capillary tube in an adiabatic wick section. The iteration process does not wait for convergence [15], the flow type is transient and requires a time step accuracy of 1, with a total simulation time of 3000 for each unit.

3. RESULTS AND DISCUSSION

The simulation results of the fluid temperature contour in the evaporator section are shown in Figs. 5-7.

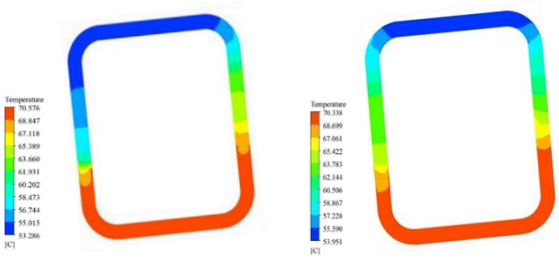

Fig. 5. Temperature contour with hot water temperature of 70 °C.

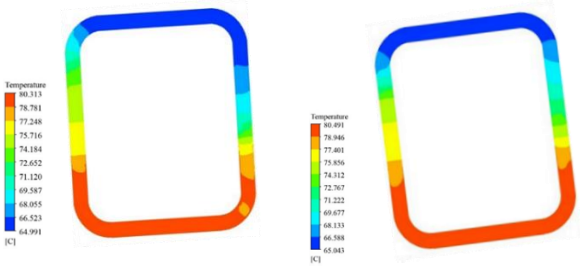

Fig. 6. Temperature contour with hot water temperature of 80 °C.

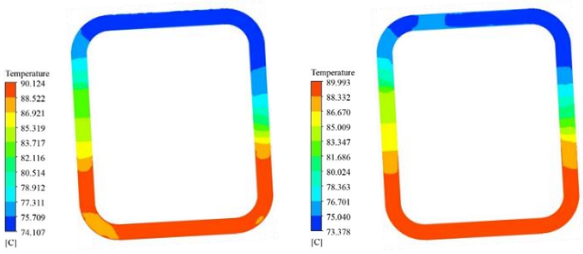

Fig. 7. Temperature contour with hot water temperature of 90 °C.

In Fig. 5, it can be observed that at the beginning of the simulation, the evaporator temperature is at 70 °C. Then, the temperature decreases to 67 °C at the beginning of the adiabatic section and reaches 61 °C at the end of the adiabatic section. In the condenser section, the temperature further decreases to 55 °C and exits at 53 °C. As it enters the adiabatic wick section, the temperature of the LHP tends to decrease. This is due to the condensate that accumulates in the condenser section flowing down to the evaporator section through the adiabatic wick.

In Fig. 6, the evaporator temperature starts at 80 °C, decreasing to 75 °C at the beginning of the adiabatic section, and further to 69 °C at the end of the adiabatic section. In the condenser section, the temperature decreases to 67 °C and exits at 67 °C. As it enters the adiabatic wick section, the temperature of the LHP tends to increase. This is because the heat from the evaporator section rises to the condenser section through the adiabatic wick.

Figure 7 shows the evaporator temperature was starting at 89 °C, then decreasing to 86 °C at the beginning of the adiabatic section, and further to 76 °C at the end of the adiabatic section. In the condenser section, the temperature decreases to 75 °C and exits at 73 °C. As it enters the adiabatic wick section, the LHP temperature tends to increase. This increase occurs because heat from the evaporator section rises to the condenser section through the adiabatic wick.

From Figs. 6–7, the distribution of the temperature profile along the LHP is presented with various hot water temperatures of 70 °C, 80 °C, and 90 °C. An escalation in the evaporator temperature leads to the vaporization of the working fluid, causing it to move towards the adiabatic section and condenser section [15]. The temperature difference between the evaporator and condenser, which tends to remain constant, is referred to as the steady phase.

In general, the observed phenomenon involves the working fluid experiencing a temperature increase due to the heat applied to the LHP wall in the evaporator section. Subsequently, the working fluid evaporates because the initial pressure in the LHP is below atmospheric pressure. The evaporated working fluid then moves toward the condenser section, where it is cooled by the temperature of the LHP condenser wall. As a result of the cooling process in the condenser, water vapor condenses and moves towards the adiabatic wick section due to the inclined angle and gravitational effects on the LHP. The presence of a capillary wick within the LHP provides a pathway for both vapor and condensate, preventing vapor from reaching the condenser via the adiabatic wick section to maintain the stability of the LHP flow. The temperature distribution contours along the length of the LHP can be seen in the Fig. 8.

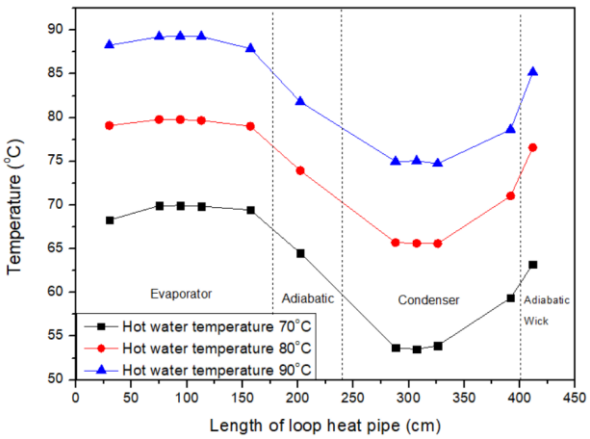

Fig. 8. Temperature distribution on various hot water temperatures.

Figure 8 illustrates the temperature distribution along the entire length of the LHP. Applying a higher heat load to the evaporator increases temperatures in both the evaporator and condenser. This also enhances heat transfer from the evaporator wall to the working fluid, consequently increasing steam generation through the boiling process. Under natural circulation, the steam flows to the adiabatic section and is then cooled in the condenser. After the temperature drops in the condenser, it rises again in the adiabatic wick section due to steam flowing from the evaporator.

Under steady-state conditions, a consistent pattern emerges across various applied heat loads. This phenomenon demonstrates that increasing the heat load on the evaporator not only accelerates the temperature of the working fluid but also raises its saturation temperature. Furthermore, a higher heat load results in more steam being transported to the condenser and a greater quantity of condensate being transferred back to the evaporator [20].

Figure 9 shows the contour of the boiling volume fraction in LHP at a hot water temperature of 70 °C and a simulation time of 1-5 seconds.

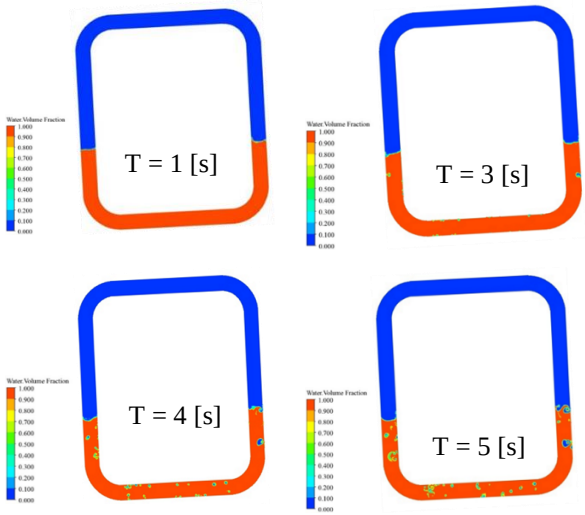

Fig. 9. Distribution of volume fraction on filling ratio 100% and hot water temperature 70 °C.

In Fig. 9, the red color indicates the presence of the working fluid in its water phase (with a water volume fraction = 1). The blue color represents the vapor phase. Initially, the working fluid in the evaporator is subjected to consistent heating at a temperature of 70 °C, simulating the heat generated by steam boiling in the pool. At some points on the evaporator's wall, the temperature becomes hotter than expected, causing vapor to form close to the wall between the 3rd and 5th seconds of the simulation. Initially, these vapor bubbles adhere to the pipe's surface [21, 22]. As the evaporator continues to heat up, these small bubbles grow into larger ones. Due to factors such as fluid dynamics and buoyancy, these bubbles tend to move along the wall, then they break away and rise to the surface of the fluid where they burst.

It can be observed that the CFD simulation visualizes the distribution of heat transfer across every part of the LHP. Furthermore, it can illustrate boiling phenomena resulting from the heating of the working fluid and the flow characteristics within the LHP. This capability enriches the study of contours and boiling phenomena that are difficult to capture through experimental methods. This modeling can be utilized to determine the profiles of temperature distribution and flow in LHP of the same dimensions under various thermal conditions

5. CONCLUSION

The CFD simulation results demonstrate the temperature distribution profile under steady-state conditions in the loop heat pipe is almost uniform at each set heating temperature in the evaporator: 70° C, 80 °C, and 90 °C.

The temperature rise in the evaporator section accelerates the boiling of the working fluid, leading to increased vapor generation from the boiling process. Due to the significant vapor production in the evaporator section, the average temperature in this region will also increase. In the adiabatic section, the temperature begins to decrease due to heat insulation. In the condenser section, the temperature decreases due to cooling and then moves towards the adiabatic wick section before returning to the evaporator.

As a result, the visualization results show the movement of steam and condensate flows during natural circulation at different hot water temperatures through CFD simulation. It can be seen that a two-phase flow rises from the evaporator to the condenser section, and condensate flows from the condenser back to the evaporator. As a future endeavor, there is a need to construct a CFD model with a User-Defined Function to simulate the WHP to simulate more advanced evaporation and condensation phenomena. Additionally, there is a need for an analysis involving transient simulations that can compare the experimental outcomes with CFD simulations to obtain the thermal resistance of the LHP.

ACKNOWLEDGMENT

The authors express their gratitude for the financial support from the “Program Pendanaan Riset dan Inovasi untuk Indonesia Maju Gelombang-1 BRIN” and acknowledge the support of the management of PRTRN-BRIN for supporting this research activity.

AUTHOR CONTRIBUTION

Restiawan, Kusuma, Rozi, and Yunus contributed as the main contributors to this paper. All authors read and approved the final version of the paper.

NOMENCLATURE

C_p	=	specific heat ($J/kg \cdot K$)
$\boldsymbol{S}_{\mathrm{CSF}}$	=	Source term of continuum surface force
g	=	gravity (m/s^2)
k	=	thermal conductivity ($W/m \cdot K$)
p	=	pressure (Pa)
S_E	=	source term of energy
S_m	=	source term of mass
t	=	time (s)
T	=	temperature (K)
$\bar{v}$	=	velocity vector (m/s)
$\bar{\bar{\tau}}$	=	stress tensor (Pa)
ρ	=	density (kg/m^3)

REFERENCES

1. Liun E. Dampak Peralihan Massal Transportasi Jalan Raya Ke Mobil Listrik. Jurnal Pengembangan Energi Nuklir. 2018. **19**(2):113.
2. Asmara, Qiqi Evaluasi Kebijakan Proses Pembangunan PLTN di Semenanjung Muria Kabupaten Jepara Jawa Tengah. Jurnal Ilmiah Neo Politea. 2020. **1**(1):31–41.
3. Saidi K., Omri A. Reducing CO2 Emissions in OECD Countries: Do Renewable and Nuclear Energy Matter? Progress in Nuclear Energy. 2020. **126**(May):103425.
4. Maemunah I.R., Yuningsih N., Irwanto D. Studi Komparasi Reaksi Fisi dan Fusi pada Pembangkit Listrik Tenaga Nuklir Masa Depan. Prosiding Seminar Nasional Fisika 5.0. 2019. **0**:473–81.
5. Suman S. Hybrid Nuclear-renewable Energy Systems: A Review. Journal of Cleaner Production. 2018. **181**:166–77.
6. Herawati N., Sudagung A.D. Persepsi Masyarakat dan Potensi Public Acceptance Terkait Wacana Pembangunan PLTN di Kabupaten Bengkayang. Jurnal Pengembangan Energi Nuklir. 2020. **22**(2):111.
7. Xie Y., Peng Y., Yuksel S., Dincer H., Uluer G.S., Caglayan C., et al. Consensus-based Public Acceptance and Mapping of Nuclear Energy Investments using Spherical and Pythagorean Fuzzy Group Decision-making Approaches. IEEE Access. 2020. **8**:206248–63.
8. Kusuma M.H. Laporan Teknis Hasil Penelitian Tahun 2019 Lembaran Kontrol Laporan Teknis Hasil Penelitian Studi Eksperimental Model Loop Heat Pipe Sebagai Sistem Pendingin Pasif di Kolam. 2019.
9. Fadillah R., Kusuma M.H., Giarno, Kholil A. Studi Pengaruh Filling Ratio Terhadap Unjuk Kerja Termal Model Loop Heat Pipe. SIGMA EPSILON-Buletin Ilmiah Teknologi Keselamatan Reaktor Nuklir. 2021. **25**(2):65–73.
10. Maydanik Y.F., Vershinin S. V., Chernysheva M.A. Investigation of Thermal Characteristics of a Loop Heat Pipe in a Wide Range of External Conditions. International Journal of Heat and Mass Transfer. 2020.
11. Harun M.A. Bin, Gunnasegaran P.A. /L, Sidik N.A.C., Beriache M., Ghaderian J. Experimental Investigation and Optimization of Loop Heat Pipe Performance with Nanofluids. Journal of Thermal Analysis and Calorimetry. 2021. **144**(4):1435–49.
12. Hadi Kusuma M., Giarno, Haryanto D., Hatmoko S., Dwi Setyo Pambudi Y., Loren ButarButar S., et al. Experimental Investigation of Thermal Characteristics on a New Loop Pipe Model for Passive Cooling System. Thermal Science and Engineering Progress. 2024. **50**:102555.
13. Suresh J.V., Bhramara P. CFD Analysis of Copper Closed Loop Pulsating Heat pipe. Materials Today: Proceedings. 2018. **5**(2):5487–95.
14. Höhne T. CFD Simulation of a Heat Pipe Using the Homogeneous Model. International Journal of Thermofluids. 2022. **15**:100163.
15. Rosidi A., Haryanto D., Wahanani N.A., Dwi Y., Pambudi S., Serpong K.P., et al. The Simulation of Heat Transfers and Flow Characterization on Wickless Loop Heat Pipe. 2022. **20**(1):29–35.
16. ANSYS Ansys Fluent Theory Guide. 2021.
17. Mathry A.H., Al-Mousawi F.N., Dhaidan N.S., Alammar A.A. Numerical Simulation of the Heat Transfer Characteristics of a Thermosyphon Heat Pipe with Different Tilt Angles and Filling Ratios. 2023. **03**(04)
18. Guichet V., Delpech B., Jouhara H. International Journal of Heat and Mass Transfer Experimental Investigation, CFD and Theoretical Modeling of Two-phase Heat Transfer in a Three-leg Multi-channel Heat Pipe. 2023. **203**
19. Narendra G., Charishma K.T.S. Materials Today: Proceedings CFD study on the Effect of Nanofluids in Natural Circulation Loop. Materials Today: Proceedings. 2022. **49**:2116–23.
20. Kusuma M.H., Putra N., Antariksawan A.R., Koestoer R.A., Widodo S., Ismarwanti S., et al. Passive Cooling System in a Nuclear-spent Fuel Pool using a Vertical Straight Wickless-heat Pipe. International Journal of Thermal Sciences. 2018. **126**(October 2017):162–71.
21. Yue C., Zhang Q., Zhai Z., Ling L. CFD Simulation on the Heat Transfer and Flow Characteristics of a Microchannel Separate Heat Pipe under Different Filling Ratios. Applied Thermal Engineering. 2018. **139**:25–34.
22. Wang K., Hu C., Cai Y., Li Y., Tang D. Investigation of Heat Transfer and Flow Characteristics in Two-phase Loop Thermosyphon by Visualization Experiments and CFD Simulations. International Journal of Heat and Mass Transfer. 2023. **203**:123812.